Unclassified
SECURITY CLASSIFICATION OF THIS PAGE

(2)

REPORT DOCUMENTATION PAGE

1 AD-A234 921

1b RESTRICTIVE MARKINGS
None

3 DISTRIBUTION/AVAILABILITY OF REPORT
Approved for public release and sale.
Distribution unlimited.

4. PERFORMING ORGANIZATION REPORT NUMBER(S)
ONR Technical Report No. 23

5. MONITORING ORGANIZATION REPORT NUMBER(S)

6a NAME OF PERFORMING ORGANIZATION
University of Utah

6b OFFICE SYMBOL (If applicable)

7a NAME OF MONITORING ORGANIZATION

6c ADDRESS (City, State, and ZIP Code)
Department of Chemistry
Henry Eyring Building
Salt Lake City, UT 84112

7b ADDRESS (City, State, and ZIP Code)

8a NAME OF FUNDING/SPONSORING ORGANIZATION
Office of Naval Research

8b OFFICE SYMBOL (If applicable)

9 PROCUREMENT INSTRUMENT IDENTIFICATION NUMBER
N00014-89-J-1412

8c ADDRESS (City, State, and ZIP Code)
Chemistry Program, Code 1113
800 N. Quincy Street
Arlington, VA 22217

10 SOURCE OF FUNDING NUMBERS

PROGRAM ELEMENT NO	PROJECT NO	TASK NO	WORK UNIT ACCESSION NO

11 TITLE (Include Security Classification)
Raman Spectroscopy Study of Solvation Structure in Acetonitrile/Water Mixtures

12 PERSONAL AUTHOR(S)
K. L. Rowlen and J. M. Harris

13a TYPE OF REPORT	13b TIME COVERED	14 DATE OF REPORT (Year, Month, Day)	15 PAGE COUNT
Technical	FROM 6/90 TO 5/91	April 22, 1991	14

16 SUPPLEMENTARY NOTATION

17 COSATI CODES			18 SUBJECT TERMS (Continue on reverse if necessary and identify by block number)
FIELD	GROUP	SUB-GROUP	Mixed solvent structure; Raman spectroscopy

19 ABSTRACT (Continue on reverse if necessary and identify by block number)

Attached.

DTIC
S

20 DISTRIBUTION/AVAILABILITY OF ABSTRACT
☒ UNCLASSIFIED/UNLIMITED ☐ SAME AS RPT ☐ DTIC USERS

21 ABSTRACT SECURITY CLASSIFICATION
Unclassified

22a NAME OF RESPONSIBLE INDIVIDUAL	22b TELEPHONE (Include Area Code)	22c OFFICE SYMBOL
Joel M. Harris	(801)581-3585	

DD FORM 1473, 84 MAR 83 APR edition may be used until exhausted
All other editions are obsolete

SECURITY CLASSIFICATION OF THIS PAGE
Unclassified

91 4 30 013

OFFICE OF NAVAL RESEARCH

Grant No: N00014-89-J-1412

R&T Code 413a005---03

Technical Report No. 23

Raman Spectroscopy Study of Solvation Structure in Acetonitrile/Water Mixtures

Prepared for publication in Analytical Chemistry

by

K. L. Rowlen and J. M. Harris

Departments of Chemistry
University of Utah
Salt Lake City, UT 84112

April 22, 1991

UNIT NO 998 010319
Gal. 1 AC5B11 AC900762K Vo63 I010

TTL03

Raman Spectroscopic Study of Solvation Structure in Acetonitrile/Water Mixtures

ADR03

AUT03 **Kathy L. Rowlen[1] and Joel M. Harris***

AAS03 *Department of Chemistry, University of Utah, Salt Lake City, Utah 84112*

ABS03

SEN03 **Raman spectroscopy is used to probe the CN stretching frequency of acetonitrile as a function of concentration in water. The CN band is modeled as the sum of two Gaussians. The concentration dependence of area and width for each of the Gaussian components provides experimental support of an equilibrium between two forms of acetonitrile in solution. In addition the concentration dependence of each of the bands correlates well with the thermodynamically related Kirkwood–Buff integrals (G_{ij}). Specifically, both the vibrational band width and G_{ij} exhibit maxima near $X_{CH_3CN} \approx 0.3$, suggestive of strong interaction between acetonitrile molecules. The frequency shift of the CN band exhibits a linear dependence on the dielectric constant of protic solvents.**

TXT03

PAR03

INTRODUCTION

SEN03 There has been considerable effort to define and understand the fundamental molecular interactions important in liquid chromatography (*1–3*). Although the solvophobic theory (*1*) is commonly invoked to explain retention in reversed-phase liquid chromatography (RPLC), recent studies have pointed out shortcomings in this model (*3, 4*). Using statistical thermodynamics, Dill (*4*) has demonstrated that retention in RPLC is driven by two classes of interactions: (1) the differences in chemical interactions of the solute in each of the phases, which affect the enthalpy of the system, and (2) changes in the entropy of the system. Studies of the importance of chemical interactions with the solvent have employed such techniques as solute solvatochromism (*5, 6*). Solvent–stationary phase interactions have also received attention (*7, 8*). It is clear that the solvent plays a crucial role in establishing the "structure" of the stationary phase, which, in turn, impacts the nature of solute retention. Recently several studies of solvent–stationary phase behavior have employed environment-sensitive probe molecules, such as pyrene, adsorbed or immobilized at the surface (*9*). Spectroscopic changes in the probe provide information about the solute but only an indirect measure of surface characteristics. An important experiment for understanding solute-induced changes in either the solvent-phase structure or the stationary-phase structure would involve monitoring some characteristic of the solvent and/or stationary phase directly. The motivation for understanding solvent structure is found in the work recently conducted by Wirth (*10, 11*), in which the importance of shape selectivity in retention (related to structural order) was demonstrated spectroscopically.

PAR06

SEN03 Acetonitrile (CH_3CN) is one of the most widely used organic modifiers in reversed-phase liquid chromatography; it also has significant application in nonaqueous electrochemistry (*12*). The Raman spectrum of CH_3CN has unique features in regions of low spectral interference; therefore, Raman spectroscopy of CH_3CN is an excellent choice for a direct probe of solvent microenvironment.

PAR09

SEN03 The CN stretch in acetonitrile exhibits a rather unique shift to higher frequency when hydrogen bonded (*13*) or coordinated with Lewis acids (*14*). On the basis of the analogous situation encountered with carbonyls, in which the CO stretch shifts to *lower* frequency when hydrogen bonded (*15*), one expects that coordination of the nitrogen lone pair electrons would lengthen and thus weaken the CN bond. In the case of carbonyls, ^{13}C nuclear magnetic resonance (NMR) studies show an apparent reduction in electron density (a shift to lower fields) about the carbonyl carbon and presumably an accompanying increase in electron density about oxygen, as the concentration of a hydrogen bond donor is increased (*16*). Similarly, NMR studies of CH_3CN–water mixtures show that

TXT03
PAR09

the ^{14}N resonance shifts to higher fields, an apparent increase in electron density about the nitrogen (*17*). Sadlej and Kecki (*18*) employed a modified CNDO method to study the electronic structure of acetonitrile and its complexes with metal cations. They attributed the increased force constant of the CN bond to a rehybridization in which the 2p σ character of the lone pair is increased. Consideration of the partial antibonding character of nitrogen's 2p σ orbital led to the conclusion that the removal of the lone pair electrons enhances the CN bond order. The authors observed that the corresponding restructuring of π electrons would account for the increased electron density about N (as measured by NMR). An increase in the force constant of the CN bond readily accounts for the observed shift to higher frequencies when CH_3CN is hydrogen bonded (*13*, *19*).

PAR12

The liquid structure of CH_3CN is also of interest and remains unresolved. Strong molecular interactions must account for the high boiling point of CH_3CN (82 °C) as well as the fact that ν_{CN} is 13 cm^{-1} higher in the gas phase than in liquid (*20*). For comparison, the boiling point of methanol (similar density and molecular weight), which exists as a hydrogen-bonded network in solution, is only 64.7 °C. It has been proposed that a liquid-phase antiparallel alignment of two CH_3CN molecules would result in a reduced dipole moment, therefore a weaker CN bond (*21*). This concept is supported by the observation that a single CH_3CN molecule in the gas phase has a dipole moment of 3.92 D, whereas the gaseous dimer has a dipole moment of 2.67 D (*14*). There is a large body of work that suggests that CH_3CN is partitioned between monomers and dimers in solution (*14*, *20*, *22*). Griffiths (*23*) indicated that it is unreasonable to expect a true CH_3CN dimer to exist in solution and that free or unassociated CH_3CN is likely to be in equilibrium with some undefined self-associated form of CH_3CN. Temperature-dependent studies of CH_3CN in a variety of solvents appear to indicate that monomeric or free CH_3CN does not exist in solution; rather, CH_3CN is organized as aggregates or loosely defined clusters (*24*). Several researchers have reported that the CN stretching band of CH_3CN in the liquid phase is composed of two overlapped Gaussians: a narrow band, attributed to the monomeric or free form of CH_3CN, and a broad band, attributed to some organized form of CH_3CN (*13*, *23*, *24*). Infrared matrix isolation studies of CH_3CN show two resolved bands in the CN stretching region (*14*)

PAR15

In order to employ CH_3CN and Raman spectroscopy as a direct probe of solute/solvent or solvent/stationary phase interactions, it is first necessary to understand the nature of vibrational perturbations arising from solvent/solvent interactions. Here we report a detailed Raman spectroscopic study of CH_3CN in water. Presented in this work is the behavior of the CN stretching vibration over the entire concentration range of acetonitrile/water mixtures and an exploration of the relationships between observed frequency shifts and solvent properties. Two groups have recently investigated the vibrational spectroscopy of CH_3CN/water mixtures (*13*, *19*), focusing primarily on the structural composition of water; neither group modeled the vibrational band structure. This work mathematically models the CN stretching band (ν_{CN}) as the sum of two Gaussians, whose behavior as a function of concentration supports the concept of an equilibrium between at least two distinct CH_3CN species in solution. Further support for such an equilibrium is found in the strong correlation between the CN frequency shift and the dielectric constant of a variety of hydrogen-bond donor solvents.

TXT06

EXPERIMENTAL SECTION

PAR18

All solvents were spectrochemical or UV grade and were stored over molecular sieves (4 Å × $\frac{1}{16}$ in.). Doubly distilled, HPLC grade (Omnisolve) water was used in all experiments involving water.

PAR21

The 514.5-nm line from an argon ion laser (Lexel Model 95) was employed as the excitation source. Plasma lines from the source were eliminated with a combination of two Pellin Brocha

TXT06
PAR21

prisms (Optics for Research, ABDU-20) and a variable aperture. The 30-mW beam was focused to approximately 80 μm at the sample cell, a 0.1- × 1-cm glass capillary (Kimax). Sample introduction was achieved via a 5-mL syringe connected to the capillary with 0.8-mm-i.d. Teflon tubing. All measurements were conducted at ambient temperature. Light from the cell was collected and collimated at 90° from excitation by a *f*/2 camera lens (Canon, fl 50 mm) and then focused at the entrance slit of the spectrograph (0.5 m, Spex 1870) with a *f*/3.9 planoconvex lens. The entrance slit width was 60 (or 80) μm in all cases, corresponding to a spectral bandwidth of 3.6 cm^{-1}. A colloidal glass (RG-530, Schott) high-pass filter, placed in front of the entrance slit, served to remove scattered source light. A 600 grove/mm grating dispersed the light across a Thomson THF7882CDA charge-coupled device (CCD, Photometrics). With the long axis (576 channels) oriented in the direction of wavelength dispersion, a spectral region of approximately 600 cm^{-1} was sampled simultaneously at approximately 1 cm^{-1}/channel. The CCD controller was linked to a Mac IIcx via a general purpose interface board (GPIB, National Instruments). The interface software, OMA, was written by Marshall Long (Yale, Applied Physics Department).

PAR24

For all spectra presented in this work, a preflash was used and the charge from 383 columns was binned along the slit axis for signal-to-noise improvement. It has recently been reported that binning in this direction can result in artificial band broadening (25). However, we are confident that the asymmetry found in the bands reported herein is physiochemical in nature based on the fact that similar band shapes have been observed and reported by workers using monochromator–PMT systems (*13*, *23*, *24*) and the following study of charge trapping conducted in this lab. The effect of charge trapping on peak parameters was quantified by using a single Lorentzian fit to the 214-cm^{-1} band of CCl_4. We found charge trapping to be of concern only at low signal intensities, <70 000 photoelectrons, in which no "preflash" had been used to uniformly irradiate the CCD. With the preflash, no band distortions were observed.

PAR27

The CH, CN, and CC stretching frequencies (2942, 2249, 918 cm^{-1}) (26) in dry CH_3CN were used as reference points for band position measurements in other solvents. These reference points were established prior to each set of measurements in a given region. To avoid mechanical backlash errors, the spectrograph settings were not varied during any group of measurements in a particular region. All quantitative measurements were made, minimally, in triplicate. Concentrations (M) were calculated taking into account the nonideal volume of mixing for CH_3CN and water, as tabulated by Katz et al. (27). Measured band areas were corrected for refractive index effects as indicated by Bauer et al. (28). The correction values vary less than 2% over the investigated concentration range.

PAR30

Data processing was conducted on an IBM AT compatible computer. Conversion of binary files from the Macintosh disk operating system to MS-DOS was carried out with the Apple File Exchange program. Peak modeling to Gaussian functions was achieved with the program Curvefit (χ^2 minimization) in SpectraCalc (Galactic Industries, V2.1). The spectra could not be modeled as Lorentzian functions.

TXT09

RESULTS AND DISCUSSION

PAR33

Acetonitrile in Water. *CN Stretch.* Figure 1 shows the CN stretching band (ν_{CN}) in neat acetonitrile. The frequency maximum shifts linearly to higher frequencies as the molar concentration of CH_3CN in water decreases, from 2249 cm^{-1} in neat CH_3CN to 2256 cm^{-1} at 1.9 M (a change of 7 ± 0.4 cm^{-1}, from eight measurements). In order to investigate the possibility and behavior of overlapped bands as a function of concentration, both ν_{CN} and ν_{II}, as labeled in Figure 1, were modeled by using the Curvefit program in Spectra Calc. ν_{II} is a combination band arising from the symmetric bend of CH_3 and the CC stretch (29). Although ν_{II} is not part of the CN stretch, it was included in the model in order to improve the accuracy of the fit. The best fit to the CN band shape is two overlapped Gaussians (ν_{II} and ν_{III}).

FIG 1 (009, 3- 4)

PAR36

Band Area. As is observed from Figure 2, the total measured area (ν_{II} + ν_{III}) is linear with concentration. Figure 3 shows the behavior of ν_{II} and ν_{III} as a function of concentration. Assuming that both ν_{II} and ν_{III} are due only to the stretching mode of CN (30), the fact that there are two bands, each

FIG 2 (006, 7 - 8)
FIG 3 (009, 3- 4)

TXT09
PAR36

having a unique concentration dependence, implies that acetonitrile exists in at least two distinct forms in solution. SEN15 Since both ν_{II} and ν_{III} are present in pure (dry) CH_3CN, neither of the two Gaussian components can be attributed to hydrogen SEN18 bonding with water. This may not be true for low concen- SEN21 trations of CH_3CN in water. Both components have nearly equivalent areas from 2 to 8 M CH_3CN which, in agreement with previous observations (*20, 24*), suggests that strong interactions between CH_3CN molecules must prevail even at SEN24 low concentrations. Between 8 and 12 M, the area of ν_{II} SEN27 increases at a rate faster than that of ν_{III}. Near 12 M (X_{CH_3CN} ≈ 0.3–0.35) CH_3CN, *there appears to be a transition between* SEN30 ν_{II} and ν_{III}. At concentrations greater than 15 M (X_{CH_3CN} ≈ SEN33 0.55), ν_{III} becomes the dominant band. The relationship between areas at concentrations greater than 12 M is consistent with a picture of the liquid in which self-associated CH_3CN, represented by ν_{III}, is favored at high concentrations.

PAR39

SEN03 Attempts to quantify a particular species, such as CH_3CN monomer or dimer, using the measured band areas were un- SEN06 successful. Substitution of activity (*31*) for molarity did not SEN09 improve the situation. However, as Pimentel and McClellan (*32*) have pointed out, one would only expect a clear, definable equilibrium between, for example, monomer and dimer in solution if the dimer were cyclic with no additional sites SEN12 available for interaction. Consideration of the data presented here and evidence that the methyl group is strongly involved in determining the structure of liquid CH_3CN (*33*) lead to the conclusion that no simple equilibrium between definite CH_3CN species exists in solution.

PAR42

SEN03 *Bandwidth.* Figure 4 shows the bandwidth (full width at SEN06 half maximum) as a function of mole fraction CH_3CN; mole fraction is used in this case, rather than molarity, to facilitate SEN09 comparison with thermodynamic parameters. Note, however, that the maximum in bandwidth occurs at the same concentration as the transition observed for band areas (≈12 M). FIG 4 (006.3-4)

PAR45

SEN03 Matteoli and Luciano (*34*) recently calculated the values of G_{ij} for CH_3CN/water mixtures from the Kirkwood-Buff integrals (*35*)

Author See MSS Page 8

$$G_{ij} = (g_{ij} - 1)4\pi r^2 \, dr \qquad (1)$$

REQU 1 (003.19-26)

where g_{ij} is the radial distribution function and r is the average SEN06 distance between adjacent molecules. G_{ij} is a measure of the tendency for dissimilar molecules to interact and G_{ii} is a SEN09 measure of interaction tendency between like molecules. G_{ij} and G_{ii} are related to thermodynamic properties as described by the following equations

$$G_{ij} = RTK_T - V_i/\bar{V}_j DV \qquad (2)$$

REQU 2 (009.15-16)

$$G_{ii} = G_{ij} + \bar{V}_j/(D - V)x_i \qquad (3)$$

REQU 3 (009.15-16)

$$D = 1 + x_i(\partial \ln \alpha_i/\partial x_i)_{TP} \qquad (4)$$

REQU 4 (009.15-16)

where R, T, K_T, $\bar{V}$, α, x_i, and V represent the gas constant, temperature, isothermal compressibility coefficient of the solution, partial molal volume, activity coefficient, mole fraction, and the volume per mole of mixture, respectively. SEN12 Matteoli and Luciano found, for both CH_3CN and water, that SEN15 G_{ii} exhibited a maximum near $X_{CH_3CN} = 0.3$ ($=X_{max}$). Such a maximum implies a strong tendency for like molecules to associate (G_{ii} vs X decreases monotonically for an ideal SEN18 mixture). On the basis of the overall shape of the G_{ii} vs X_i curve, the authors divided the solution behavior into three categories, the maximum serving as the transition between SEN21 solvation and self-association. At $X_{CH_3CN} < X_{max}$, the trend of G_{ii} for water indicated that small amounts of CH_3CN could SEN24 significantly affect the structure of water. The structure of CH_3CN remains primarily unaffected by small amounts of SEN27 water. At $X_{CH_3CN} > X_{max}$, the authors noted that the smooth trend of G_{ii} toward neat CH_3CN was suggestive of direct interaction between CH_3CN molecules.

PAR48

SEN03 The bandwidths of both ν_{II} and ν_{III} exhibit a maximum near SEN06 $X_{CH_3CN} = 0.3$. The maximum is more pronounced for ν_{III} (self-associated CH_3CN); thus, the behavior of the bandwidth

TXT09
PAR48

may be more closely associated with CH_3CN. CH_3CN interactions rather than CH_3CN/H_2O interactions. Since both the bandwidths and band areas undergo dramatic transitions at the concentrations of similar activity for the Kirkwood integrals, there appears to be a relationship between the solvent structure probed by Raman spectroscopy and the thermodynamic properties of the solution. In addition, it is interesting to note that the bandwidth maximum occurs at precisely the point at which the partial molar excess volumes of CH_3CN and water are equal (*36*). Kamagawa and Kitagawa (*33*), using Raman difference spectroscopy to analyze the symmetric CH stretch of CH_3CN in water, found that a plot of homogeneous frequency shift (the shift attributed to self-associated molecules) vs mole fraction was very similar to the plot of partial molar volume vs mole fraction. The authors interpreted this as an indication that the frequency shift was related to the structure of the solution.

PAR51

Frequency Shifts. Figure 5 shows the center frequency of $\nu_{\perp}$ and $\nu_{\parallel}$ vs mole fraction. The measured center frequency for ν_{CN} is dominated by $\nu_{\parallel}$ and therefore exhibits similar behavior. For the purpose of discussion, we will assume that an CH_3CN dimer is representative of self-associated CH_3CN. Thomas and Thomas-Orville proposed the structure of an CH_3CN dimer as

FIG 5 (006, 3- 4)

RGID AC5B11a (015,12-13)

This structure also derives from both neutron diffraction studies and ab initio calculations as the most energetically stable CH_3CN dimer orientation for intermolecular distances less than 5 Å (*22*). According to Pauling (*37*), due to the large dipole moment, the CN bond can posses as much as 21% ionic character. Bulk solvent effects, such as dielectric properties, are therefore expected to play a key role in determining the strength of inter-molecular interactions. If self-association results in a lower CN force constant, through partial cancellation of dipole moments—as mentioned in the Introduction—then the effective solvation of self-associated CH_3CN should result in an increase in ν_{CN}. Hydrogen bonding, in which the partially antibonding lone pair electrons are removed from the CN bond, should also result in an increase in ν_{CN}. Therefore, in the case of protic solvents, the magnitude of shift in ν_{CN} is expected to have a complicated dependence on both solvent dielectric properties and hydrogen-bond strength. It is worth noting that the center frequency of $\nu_{\parallel}$ exhibits a linear dependence on molarity, whereas $\nu_{\perp}$ has a more complicated dependence. The dielectric constant of CH_3CN–water mixtures varies approximately linearly with molarity (*38*). In addition to dielectric and hydrogen-bond effects, there is evidence that suggests that hydrophobic interactions may also play a role in CH_3CN aggregation at high water concentrations (*33*, *34*).

PAR54

To test the importance of dielectric effects, a study of CH_3CN (X_{CH_3CN} = 0.037, 1.9 M) in a variety of protic (hydrogen-bond donating) solvents was conducted. Figure 6 shows the frequency shift from 2249 cm^{-1} (ν_{CN} in pure CH_3CN) as a function of dielectric constant. The frequency shift for CH_3CN would, of course, be zero but is not shown on the graph because it is not a hydrogen-bond donor. Note that water (ϵ = 78.5) is the only solvent in the figure that has a higher dielectric constant than CH_3CN (ϵ = 38.8). The difference in the magnitude of shift for water and its nearest neighbor (MeOH) is significant. The linearity of the plot as well as the magnitude of the shift for water indicates a strong dependence on the dielectric properties of the solvent. Plots of frequency shift vs (1) dipole moment, (2) refractive index, (3) polarizability (calculated from the Clausius–Mossotti equation), and (4) orientation polarizability (Δf) (calculated from the Lippert equation (*40*)) were all nonlinear or uncorrelated. For the above calculations, it was assumed that the bulk properties of the mixture were equivalent to those of the solvent. This assumption is valid for dilute solutions, as is true for X_{CH_3CN} = 0.037. Although bulk dielectric properties appear to play a primary role in determining ν_{CN}, hydrogen bonding must also take place. Recent ab initio calculations have estimated

FIG 6 (006, 3- 4)

TXT09
PAR54

the hydrogen-bond strength of CH_3CN water to be approximately 4 kcal/mol (*41*). The OH stretch of water is quite sensitive to dilution with CH_3CN, shifting more than 100 cm^{-1} over the concentration range studied. The magnitude of the shift is characteristic of hydrogen-bond donors (*42*).

PAR57

Both the CC and CH stretching modes shift to higher frequency upon dilution of CH_3CN in water. The slopes of center frequency vs molarity are 0.39 and 0.27 for ν_{CC} and ν_{CH}, respectively.

PAR60

Associated Species. Katz et al. (*27*) recently suggested that mixtures of MeOH/water, CH_3CN/water, and tetrahydrofuran (THF)/water should be regarded as ternary solvent systems, the three components being free solvent (i.e., not associated with water), free water, and a solvent/water complex. The authors postulated that deviation from ideal mixing, as well as chromatographic anomolies, could be explained in terms of the presence of this third (solvent/water) species. They mathematically modeled the volume of the mixing curve by assuming that the molar volume of all three components remained constant over the entire range of compositions. However, it is well documented that the molar volume of components in nonideal solutions does indeed vary (*42*). In addition, in describing CH_3CN/water mixtures as a simple equilibrium

$$CH_3CN + H_2O \rightleftharpoons CH_3CN/H_2O$$

$$K_{eq} = [CH_3CN/H_2O]/[CH_3CN][H_2O] \qquad (5)$$

REQU 5a (018.11-12

REQU 5 (018.11-12)

the *activities* of water, CH_3CN, and CH_3CN/H_2O must be used to calculate K_{eq}. Based on the activities reported by French (*31*), the equilibrium in eq 5 would result in an $CH_3CN \cdot H_2O$ complex whose activity remains constant from 0.2 to 0.7 mole fraction CH_3CN. The model used by Katz et al. results in a continuously varying associated complex (as measured by volume fraction) that exhibits a maximum near $X_{CH_3CN} = 0.25$. Based on the results of Matteoli and Luciano (*34*), the minimum in the volume of mixing may be due to effective "packing" of CH_3CN within the water structure rather than a maximum in CH_3CN/H_2O complexes. While it is intuitively satisfying to consider associated species in binary mixtures, the model Katz et al. have chosen may not be an accurate description.

PAR63

Taking into account both solvent/solvent and solvent/solute species, CH_3CN/water mixtures are more thoroughly described as having at least six general components: $(CH_3CN)_n$, CH_3CN, $(CH_3CN)_n/H_2O$, CH_3CN/H_2O, H_2O, and $(H_2O)_n$. As the concentration is varied, the distribution of interactions must also vary. At low CH_3CN concentrations ($X_{CH_3CN} < 0.3$), due to the strength of attractive forces between CH_3CN molecules, it is not unreasonable that both free (e.g., CH_3CN, $CH_3CN \cdot H_2O$) and self-associated (e.g., CH_3CN/CH_3CN) CH_3CN exist. The stable association of CH_3CN molecules would eventually serve to disrupt the water structure. Based on the observations of Singh and Krueger (*19*), in which the 3225-cm^{-1} band in water vanishes as CH_3CN is increased to $X_{CH_3CN} = 0.47$, the structure of water appears to be dominant up to $X_{CH_3CN} = 0.3$. Beyond that point, both the structure of water and of CH_3CN approach their least structural form. The maximum excess entropy of mixing ($X_{CH_3CN} = 0.55$), rather than the volume of mixing, is likely to be correlated with the largest degree of association between CH_3CN and water (see Figure 7 (*31*, *43*)). At CH_3CN mole fractions greater than 0.55, the structure of CH_3CN dominants. This concept is supported by the fact that the area of band III, attributed to self-associated CH_3CN, becomes the dominant factor at CH_3CN mole fractions greater than 0.55.

FIG 7 (021.34-35)

PAR66

Although there are undoubtedly a variety of effects that influence the degree of association between CH_3CN molecules, it is possible that the dominant driving force for aggregation progresses from hydrophobic to electrostatic as the CH_3CN concentration is increased. At high water concentrations, the dielectric constant of the solution is high; therefore, electrostatic interactions are minimized while the tendency for hy-

TXT09
PAR66
SEN09 23 drophobic interactions is maximized. As mentioned above,
5 the shape of the G_{23} vs X_{CH_3CN} curve suggests that for X_{CH_3CN}
17 > 0.3 direct interactions between CH_3CN molecules occurs.
SEN12 1 If one defines direct interaction as that which occurs at in-
12 termolecular separation distances ≤ 5 Å, the antiparallel
20 orientation of two CH_3CN molecules is the most stable dimer
SEN15 30 (*27*). A dimer, in which the opposite partial charges are
31 aligned, seems reasonable at high CH_3CN concentrations.
SEN18 1 High CH_3CN concentrations would facilitate stronger elec-
8 trostatic attraction via decreased average intermolecular
24 distances and a lower dielectric constant.
PAR69
SEN03 1 *Chromatographic Implications.* The presence of a variety
SEN06 7 of CH_3CN species in solution would result in complicated
SEN09 16 equilibria for solvation of other solutes. Shifts in the equilibria,
6 which occur as the solvent composition is varied, may account
SEN12 16 for anomalies in chromatographic retention (*44*). McCormick
3 and Karger (*45*) have reported the adsorption isotherms for
12 MeOH, CH_3CN, and THF on a hydrophobic stationary phase
SEN15 21 (C-18). Both CH_3CN and THF exhibited dramatic maxima
4 near 50% (X_{CH_3CN} = 0.25) and 70% (v/v) organic modifier,
SEN18 19 respectively. For acetonitrile/water mixtures, more than twice
8 as much CH_3CN is adsorbed to the surface at mobile-phase
SEN21 28 composition X_{CH_3CN} = 0.25 than at X_{CH_3CN} = 0.55. In ac-
3 cordance with the solvophobic theory, the authors attributed
11 the decreased adsorption of the organic modifier to reduced
20 [illegible] concentration [illegible] being the
29 driving force for removal of organic modifier from solution.
SEN24 1 However, the removal of organic modifier from solution is
12 unlikely to be driven by entropy, since (1) the process of
22 concentrating solvent/solute at the interface is accompanied
29 by a decrease in entropy due to structuring of the alkyl phase
41 (*3*, *4*) and (2) the solvation of CH_3CN in water is purely en-
SEN27 52 tropy driven (see Figure 7). If hydrophobic expulsion were
6 exclusively responsible for concentrating CH_3CN at the sur-
13 face, the process should be most favorable when the enthalpy
SEN30 21 of mixing is least favorable, and such is not the case. As shown
4 in Figure 7, the interaction between CH_3CN and water is most
15 *endothermic* (least favorable) at mole fractions much higher
23 (X_{CH_3CN} = 0.65) than the observed maximum in the isotherm.
SEN33 1 These conclusions are in agreement with studies that suggest
11 that hydrophobic expulsion is not the dominant interaction
19 in RPLC retention (*3*).
PAR72
SEN03 1 As *mentioned previously*, Katz *et al.* (*27*) suggest that
11 anomalies in solute retention can be explained in terms of
21 associated solvent species, each of which has unique inter-
SEN06 29 actions with the stationary phase. As the mobile phase is
7 varied, the chemical characteristics of the stationary phase
15 are determined by the relative concentrations of the individual
SEN09 24 species (e.g. CH_3CN, CH_3CN/H_2O, H_2O). The spectroscopic
4 evidence presented here, in conjunction with thermodynamic
SEN12 11 considerations, supports this proposal. The activity of CH_3CN
6 in water increases drastically over the range X_{CH_3CN} = 0–0.25,
SEN15 16 at which point it levels off (*31*). Based on the area and
17 bandwidth behavior of ν_{II} and ν_{III}, the region of increasing
SEN18 28 activity may be due to changes in the ratio of hydrogen-bonded
7 to self-associated species. The minimal changes in CH_3CN
SEN21 17 activity at high CH_3CN concentrations may be due to the
3 formation of a stable self-associated CH_3CN complex. The
11 maximum in the adsorption isotherm reported by McCormick
21 and Karger (*45*) corresponds to the transition point in activity
29 and quite closely with the transition in CH_3CN microenvi-
TXT12 ronment as reported here.
SEN01 1 ## CONCLUSION
PAR75
SEN03 1 Raman spectroscopy has been used to quantify vibrational
10 frequency changes in acetonitrile under hydrogen-bond con-
SEN06 16 ditions. The CN band of acetonitrile was shown to consist
SEN09 11 of overlapped Gaussians (II and III). The behavior of bands
6 II and III as a function of concentration in water provides
17 experimental support for an equilibrium between CH_3CN
SEN12 24 species in solution. Comparison of band behavior with the
4 Kirkwood–Buff G values demonstrates a relationship between
15 solute microenvironment and the thermodynamic properties
SEN15 21 of the solution. The center frequency of the individual bands

as a function of concentration in water was discussed in terms of both dielectric and hydrogen-bond effects.

ACKNOWLEDGMENT

We thank W. R. Fawcett for helpful discussions on the electronic structure of CH_3CN and for directing us to valuable references.

LITERATURE CITED

Present Address: Department of Chemistry, University of Colorado, Boulder, CO 80309

* Address correspondence to this author

(1) Horvath, C.; Melander, W.; Molnar, I. *J. Chromatogr.* **1976**, *125*, 129.

(2) Michels, J. J.; Dorsey, J. G. *J. Chromatogr.* **1988**, *457*, 85.

(3) Dorsey, J. G.; Dill, K. A. *Chem. Rev.* **1989**, *89*, 331.

(4) Dill, K. A. *J. Phys. Chem.* **1987**, *91*, 1980.

(5) Sadek, P. C.; Carr, P. W.; Doherty, R. M.; Kamlet, M. J.; Taft, R. W.; Abraham, M. H. *Anal. Chem.* **1985**, *57*, 2971.

(6) Johnson, B. P.; Khaledi, M. G.; Dorsey, J. G. *J. Chromatogr.* **1987**, *384*, 221.

(7) Lochmuller, C. H.; Colborn, A. S.; Hunnicut, M. L.; Harris, J. M. *J. Am. Chem. Soc.* **1984**, *106*, 4077.

(8) Lochmuller, C. H.; Colborn, A. S.; Hunnicut, M. L.; Harris, J. M. *Anal. Chem.* **1983**, *55*, 1344.

(9) Carr, J. W.; Harris, J. M. *Anal. Chem.* **1986**, *58*, 626.

(10) Wirth, M. J. *J. Phys. Chem.* **1987**, *91*, 3926.

(11) Wirth, M. J.; Hahn, D. A. *J. Phys. Chem.* **1987**, *91*, 3099.

(12) Bard, A. J.; Faulkner, L. R. *Electrochemical Methods*; Wiley: Canada, 1980.

(13) Kabisch, V. G. *Z. Phys. Chem. (Leipzig)* **1982**, *263*, 48.

(14) Freedman, T. B.; Nixon, E. R. *Spectrochim. Acta* **1972**, *28A*, 1375.

(15) Nyquist, R. A. *Appl. Spectrosc.* **1990**, *44*, 426.

(16) Nyquist, R. A.; Putzig, C. L.; Hasha, D. L. *Appl. Spectrosc.* **1989**, *43*, 1049.

(17) Lowenstein, A.; Margalit, Y. *J. Phys. Chem.* **1965**, *69*, 4152.

(18) Sadlej, J.; Kecki, Z. *Rocz. Chem.* **1969**, *43*, 2131.

(19) Singh, S.; Krueger, P. J. *J. Raman Spectrosc.* **1982**, *13*, 178.

(20) Sadlej, J. *Spectrochim. Acta* **1979**, *35A*, 681.

(21) Thomas, B. H.; Thomas-Orville, W. J. *J. Mol. Struct.* **1969**, *3*, 191.

(22) LaManna, G. *Chem. Phys. Lett.* **1983**, *103*, 55.

(23) Griffiths, J. E. *J. Chem. Phys.* **1973**, *59*, 751.

(24) Lowenschuss, A.; Yellin, N. *Spectrochim. Acta* **1975**, *31A*, 207.

(25) Pemberton, J. E.; Sobocinski, R. L.; Sims, G. R. *Applied Spectrosc.* **1990**, *44*, 328.

(26) Dollish, F. R.; Fateley, W. G.; Bentley, F. F. *Characteristic Raman Frequencies of Organic Compounds*; Wiley: New York, 1973.

(27) Katz, E. D.; Ogan, K.; Scott, R. P. W. *J. Chromatogr.* **1986**, *352*, 67.

FNN29
FNP84
SEN03 (28) Bauer, J.; Brauman, J. I.; Pecora, R. *J. Chem. Phys.* **1975**, *63*, 53.
FNN30
FNP87
SEN03 (29) Addison, C. C.; Amos, D. W.; Sutton, D. *J. Chem. Soc. A* **1968**, 2287.
FNN31
FNP90
SEN03 (30) Wofford, B. A.; Bevan, J. W.; Olson, W. B.; Lafferty, W. J. *J. Chem. Phys.* **1985**, *83*, 6188.
FNN32
FNP93
SEN03 (31) French, H. T. *J. Chem. Thermodyn.* **1987**, *19*, 1155.
FNN33
FNP96
SEN03 (32) Pimentel, G. C.; McClellan, A. L. *The Hydrogen Bond*; Reinhold: New York, 1960.
FNN34
FNP99
SEN03 (33) Kamagawa, K.; Kitagawa, T. *J. Phys. Chem.* **1986**, *90*, 1077.
FNN35
FNP102
SEN03 (34) Matteoli, E.; Lepori, L. *J. Chem. Phys.* **1984**, *80*, 2856.
FNN36
FNP105
SEN03 (35) Kirkwood, J. G.; Buff, F. P. *J. Chem. Phys.* **1951**, *19*, 774.
FNN37
FNP108
SEN03 (36) Handa, Y. P.; Benson, G. C. *J. Solution Chem.* **1981**, *10*, 291.
FNN38
FNP111
SEN03 (37) Pauling, L. *The Nature of the Chemical Bond*; Cornell University Press: Ithaca, NY, 1960.
FNN39
FNP114
SEN03 (38) Akhadov, Y. Y. *Dielectric Properties of Binary Solutions*; Pergamon Press: New York, 1981.
FNN40
FNP117
SEN03 (39) Weast, R. C., Ed. *Handbook of Chemistry and Physics*, 62nd ed.; CRC: Boca Raton, FL, 1981.
FNN41
FNP120
SEN03 (40) Lakowicz, J. R. *Principles of Fluorescence Spectroscopy*; Plenum Press: New York, 1983.
FNN42
FNP123
SEN03 (41) Damewood, J. R.; Kumpf, R. A. *J. Phys. Chem.* **1987**, *91*, 3449.
FNN43
FNP126
SEN03 (42) Moreau, C.; Douheret, G. *Thermochim. Acta* **1975**, *13*, 385.
FNN44
FNP129
SEN03 (43) Christensen, J. J.; Rowley, R. L.; Izatt, R. M. Eds. *Handbook of Heats of Mixing*; Wiley: New York, 1988.
FNN45
FNP132
SEN03 (44) Reymond, C.; Chung, G. N.; Mayer, J. M.; Testa, B. *J. Chromatogr.* **1987**, *391*, 97.
FNN46
FNP135
SEN03 (45) McCormick, R. M.; Karger, B. L. *Anal. Chem.* **1980**, *52*, 2249.
RCP03

SEN03 RECEIVED for review September 24, 1990. Accepted February
SEN09 25, 1991. This work was supported in part by the Office of
Naval Research.

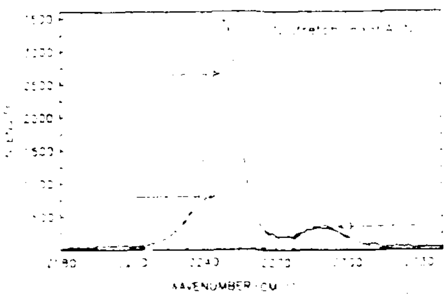

AP00 **Figure 1** CN stretch (2249 cm⁻¹) in neat acetonitrile with a 10-s
AP06 integration time. The dashed lines represent the modeled Gaussians.
AP09 The data are unsmoothed.

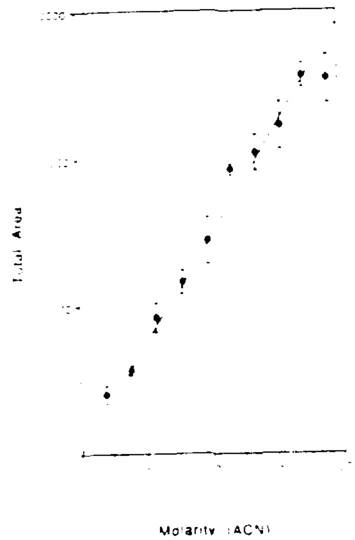

AP00 **Figure 2** Total area as a function of concentration; error bars are
AP06 ±σ. The equation for the line in y = 1458 (±34).

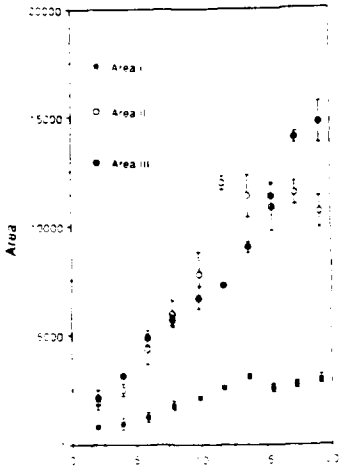

AP00 1
AP06 11
10

Figure 3 Area of individual Gaussian components as a function of CH_3CN molarity. In some cases, the symbol width exceeds the measured error.

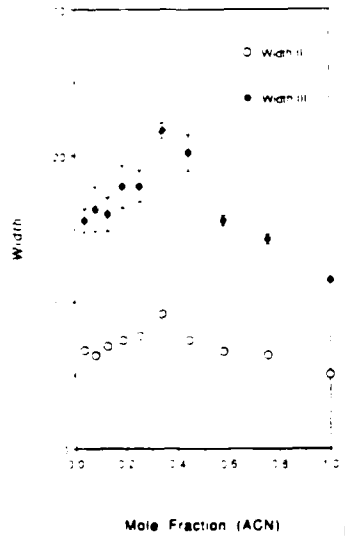

AP00 1
AP06 11
9

Figure 4 Bandwidth (full width at half-maximum) as a function of concentration; error bars are $\pm\sigma$. For band II, the symbol width is larger than the measured error.

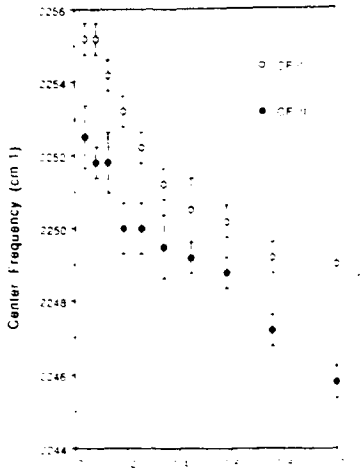

CAP00 . **Figure 5** Center frequency as a function of concentration; error bars
CAP03 11 are $\pm\sigma$

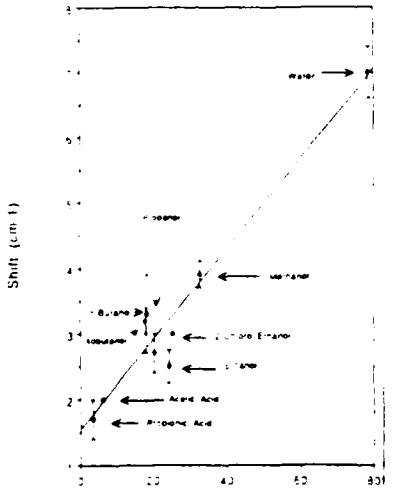

CAP00 1 **Figure 6** Shift, in cm1-, from 2249 cm^{-1} for 1.9 M CH_3CN in a variety
CAP06 15 of protic solvents. The error bars are $\pm\sigma$ from a minimum of three
CAP09 12 replicate measurements. The linear equation is $y = 1.5 + 0.089x$,
CAP12 11 $R = 0.97$. All dielectric constant values were taken from ref 39

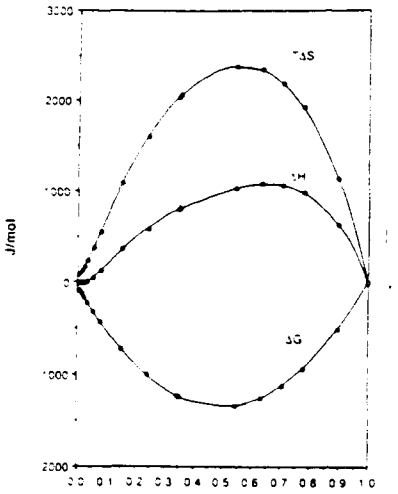

CAP00 : **Figure 7** Excess thermodynamic properties of the CH_3CN/water
CAP06 : mixture ΔH^E from ref 43 and ΔG^E from ref 31.

The number of words in this manuscript is 5308.

The manuscript type is A

Author Index Entries

Rowlen, K. L.

Harris, J. M.

Text Page Size Estimate = 4.5 Pages

Graphic Page Size Estimate = 1.3 Pages

Total Page Size Estimate = 5.8 Pages